

CIMON: Towards High-quality Hash Codes

Xiao Luo^{12*}, Daqing Wu^{12*}, Zeyu Ma³, Chong Chen^{12†}
 Huasong Zhong², Minghua Deng¹, Jianqiang Huang², Xian-sheng Hua²

¹School of Mathematical Sciences, Peking University

²Damo Academy, Alibaba Group

³College of Engineering and Computer Science, Australian National University

{xiaoluo, wudq, dengmh}@pku.edu.cn, {cheung.cc, huasong.zhs, jianqiang.hjq, xiansheng.hxs}@alibaba-inc.com, ma.zeyu@foxmail.com

Abstract

Recently, hashing is widely-used in approximate nearest neighbor search for its storage and computational efficiency. Due to the lack of labeled data in practice, many studies focus on unsupervised hashing. Most of the unsupervised hashing methods learn to map images into semantic similarity-preserving hash codes by constructing local semantic similarity structure from the pre-trained model as guiding information, i.e., treating each point pair similar if their distance is small in feature space. However, due to the inefficient representation ability of the pre-trained model, many false positives and negatives in local semantic similarity will be introduced and lead to error propagation during hash code learning. Moreover, most of hashing methods ignore the basic characteristics of hash codes such as collisions, which will cause instability of hash codes to disturbance. In this paper, we propose a new method named Comprehensive sImilarity Mining and cOnsistency learNing (CIMON). First, we use global constraint learning and similarity statistical distribution to obtain reliable and smooth guidance. Second, image augmentation and consistency learning will be introduced to explore both semantic and contrastive consistency to derive robust hash codes with fewer collisions. Extensive experiments on several benchmark datasets show that the proposed method consistently outperforms a wide range of state-of-the-art methods in both retrieval performance and robustness.

Introduction

Hashing-based Approximate Nearest Neighbour (ANN) search has attracted ever-increasing attention in the era of big data due to their high retrieval efficiency and low storage cost. The main idea of hashing methods is to project high dimensional datapoints into compact binary codes while preserving the semantic similarity of original datapoints.

Hashing methods can be subdivided into supervised hashing (Luo et al. 2020; Li et al. 2017; Cao et al. 2018) and unsupervised hashing. However, supervised hashing methods are difficult to be applied in practice since large-scale data annotations are unaffordable. To address this problem, several deep learning-based unsupervised methods were pro-

*Equal Contribution. This work is done when Xiao Luo and Daqing Wu both work as full-time research intern at Damo Academy.

†Corresponding Author.

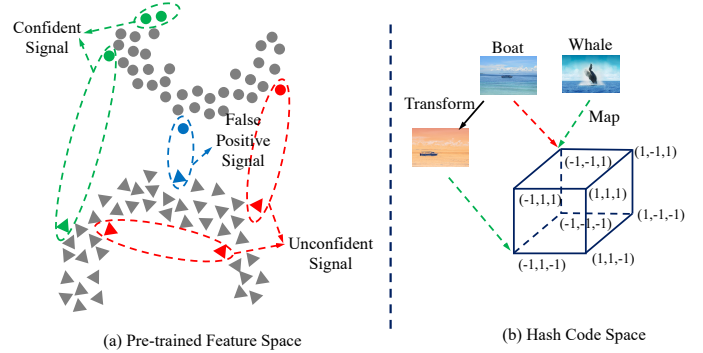


Figure 1: Motivation of our model. (a) The “triangle” points and the “circle” points are belong to different categories. False signals (blue) and unconfidence signals (red) will misguide the hash code learning. (b) Two different images (the first line) are mapped to the same hash code (collision) and the hash code is sensitive to the transformation, which implies the hash code is of low quality.

posed and provided a cost-effective solution for more practical applications (Krizhevsky, Hinton et al. 2009; Lin et al. 2016; Yang et al. 2018, 2019; Tu, Mao, and Wei 2020). Recently, most of the unsupervised hashing methods employ a two-step framework: Firstly, local semantic similarity structure is reconstructed from the pre-trained neural network. To be specific, the local semantic similarity relationships are often derived from the Euclidean distance or the cosine similarity of deep features extracted from the pre-trained model. Secondly, a hashing network is optimized to generate compact and similarity-preserving hash codes by incorporating the defined similarity structure as guiding information.

However, the existing methods have two significant drawbacks that will harm the quality of hash codes. First, many false positives and negatives will be introduced in similarity matrix for the inefficient representation ability of the pre-trained model, which will misguide the hashing model during hash code learning and further damage the retrieval performance. As shown in Figure 1(a), false similar pairs can occur between the boundary points of two manifolds (blue points). Moreover, most methods treat the confident sig-

nals and uncofident signals equally (green and red points), which will also accumulate a lot of errors. Second, they ignore the basic characteristics of hash codes such as collisions, which will lead to unstable hash codes and greatly influence the quality. For example, images of different classes with similar background could be mapped to the same hash code while the transformed image could be quite far away from the origin image in hash code space (Figure 1(b)).

To address the above two issues, we propose a new method named CIMON, which comprehensively explores semantic similarity structure to achieve reliable semantic guidance and considers the basic characteristics of hash codes by introducing consistency learning. Specifically, CIMON firstly takes advantage of global information to remove false positives between boundary points and smooths the unconfident signals by confidence adjustment. Secondly, CIMON generates two groups of deep features by data augmentation and constructs two similarity matrices and both parallel semantic consistency and cross semantic consistency are encouraged to generate robust hash codes. Furthermore, contrastive consistency between hash codes are also encouraged to generate robust hash codes with fewer collisions. Through these improvements, CIMON could help to obtain high-quality hash codes in both retrieval performance and robustness, which is also demonstrated by extensive experiments on several challenging benchmark datasets. Our main contributions can be summarized as following:

- CIMON not only utilizes global constraint learning to refine the initial local semantic similarity structure, but also explores the similarity statistical distribution to adjust the weight for each image pair based on confidence, which generates reliable and smooth guidance for hash code learning.
- A novel consistency loss including semantic consistency and contrastive consistency is proposed to optimize the hashing network, which helps to generate robust and discriminative hash codes with fewer collisions.
- Experiments on several popular benchmark datasets show that our method outperforms current state-of-the-art unsupervised hashing methods by a large margin.

Related Work

Deep Unsupervised Hashing. Unsupervised deep hashing methods usually use deep features to construct semantic structure, by which unsupervised problems can be turned into supervised problems. In a quite different way, DeepBit (Lin et al. 2016) regards the original images and the corresponding rotated images as similar pairs and tries to preserve the similarities when learning related hash codes. Stochastic generative hashing (Dai et al. 2017) tries to learn hash functions by using a generative model based on the minimum description length principle. Semantic Structure-based Unsupervised Deep Hashing(SSDH) (Yang et al. 2018) uses a specific truncated function on the pairwise distances and constructs the similarity matrices. The model is then trained by deep supervised hashing methods. DistillHash (Yang et al. 2019) improves the performance of SSDH by distilling

the data pairs with confident similarity signals. Clustering-driven Unsupervised Deep Hashing (Gu et al. 2019) recursively learns discriminative clusters by soft clustering model and produces binary code with high similarity responds. MLS³RDUH (Tu, Mao, and Wei 2020) further utilizes the intrinsic manifold structure in feature space to reconstruct the local semantic similarity structure, and achieves the state-of-the-art performance.

Contrastive Learning. (Hadsell, Chopra, and LeCun 2006) is the first work to learn representations by contrasting positive pairs against negative pairs. To solve the storage of large scale dataset, (Wu et al. 2018) proposes to utilize a memory bank for class representation vectors. Various pretext work is based on several forms of contrastive loss function, which is related to the exemplar-based task and noise-contrastive estimation (Dosovitskiy et al. 2014). Recently, Momentum Contrast (He et al. 2020) proposes to build a dynamic dictionary with a queue and a moving-averaged encoder, which enables building a large and consistent dictionary on-the-fly that facilitates contrastive unsupervised learning. SimCLR (Chen et al. 2020) further simplifies the learning algorithms without requiring specialized architectures or a memory bank and achieves better performance on ImageNet.

The Proposed Model

In this section, we first formally define the problem and feature our model with two parts as shown in Figure 2:

- **Semantic information generating.** A pre-trained VGG-F (Simonyan and Zisserman 2015) without the last fully-connected layer $F(\cdot)$ is adopted to extract deep features, which will be used to generate similarity graph and confidence-based weight matrix.
- **Consistency learning.** The hashing network $G(\cdot)$ is modified from VGG-F by replacing the last fully-connected layer with a fully-connected layer with L hidden units to incorporate the hash code learning process. We adopt a novel consistency learning framework to learn high-quality hash codes.

Problem Formulation

In the problem of deep unsupervised hashing, $\mathcal{X} = \{x_i\}_{i=1}^N$ denotes the training set with N samples without label annotations, it aims to learn a hash function

$$\mathcal{H} : x \rightarrow b \in \{-1, 1\}^L,$$

where x is the input sample and b is a compact L -bit hash code. This map should preserve similarity, i.e., images with similar ground truth labels should correspond to hash codes with small Hamming distances.

Semantic Information Generating

In our model, semantic information is composed of the similarity pseudo-graph and the similarity confidence matrix.

From the local perspective, the pseudo-graph is used to capture pairwise similarity information. Based on the pre-trained deep features $\{F(x_i)\}_{i=1}^N$, the cosine distance between the i -th and the j -th samples can be computed by

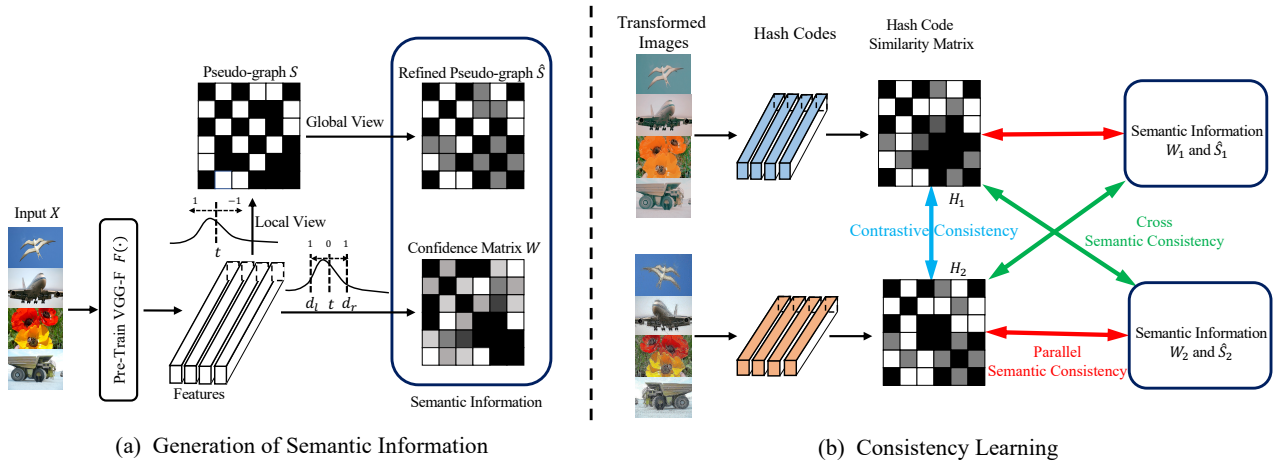


Figure 2: Overview of CIMON. (a) CIMON generates semantic information including refined pseudo-graph and confidence matrix for reliable guidance. (b) With data augmentation, CIMON generates two groups of semantic information. The parallel and cross semantic consistency is constructed between features and hash codes under the same group and crossing the different groups respectively. The contrastive consistency is based on two groups of hash codes.

$d_{ij} = 1 - \frac{F(x_i) \cdot F(x_j)}{\|F(x_i)\|_2 \|F(x_j)\|_2}$. We set a large threshold t , and consider data points with the cosine distance smaller than t as potential similar ($S_{ij} = 1$) and data points with the cosine distance larger than t as potential dissimilar ($S_{ij} = -1$). Based on the threshold t , we construct the pseudo-graph S as:

$$S_{ij} = \begin{cases} 1 & d_{ij} \leq t, \\ -1 & d_{ij} > t \end{cases} \quad (1)$$

Global Refinement Then we introduce a global constraint to refine the semantic similarity via approximate optimization. Naturally, semantic similar structure should satisfy three essential rules: reflexivity, symmetry and transitivity. The first two rules obviously hold. However, transitivity doesn't always hold in pseudo-graph S (e.g. $S_{ij} = S_{jk} = 1$, $\Rightarrow x_i$ is similar to x_k). Therefore, we refine pseudo-graph S as \hat{S} , which is estimated by finding the most similar matrix to S under transitivity rule. In formulation,

$$\begin{aligned} \min_{\hat{S}} \quad & \sum_{i,j} |\hat{S}_{ij} - S_{ij}| \\ \text{s.t.} \quad & \hat{S}_{ii} = 1, \hat{S}_{ij} = \hat{S}_{ji} \quad \forall i, j \\ & g(\hat{S}) = \text{True} \end{aligned} \quad (2)$$

in which $g(\hat{S}) = \text{True}$ implies \hat{S} meets the transitivity rule: $S_{ij} = S_{jk} = 1, \Rightarrow S_{ik} \geq 0, \forall i, j, k$.

It is unrealistic to achieve the optimal solution of Equation 2 since it is NP-hard. However, we can obtain an approximate solution by taking advantage of global information from spectral clustering (Zelnik-manor and Perona 2005). Specifically, assume $c_i \in \{1, \dots, K\}$, $i = 1, \dots, N$ is the i -th cluster label of spectral clustering (K is the number of clusters), then the refined pseudo-graph \hat{S} is formulated as :

$$\hat{S}_{ij} = \begin{cases} 1 & c_i = c_j \& S_{ij} = 1 \\ -1 & c_i \neq c_j \& S_{ij} = -1 \\ 0 & \text{otherwise} \end{cases} \quad (3)$$

Note that spectral clustering starts from the pairwise similarity and preserves most of the local semantic information while satisfying the global constraint. Specifically, \hat{S} meets the conditions in Equation 2 and is consistent with the original S . Moreover, it is easy to check that the false positives and negatives between the boundary points can be removed after our global refinement.

Confidence Adjustment Note that the semantic confidence of similarity signal for each pair is different, we further construct the confidence matrix for pseudo-graph S based on the semantic confidence. By observing the distribution of cosine distances for deep feature pairs, we find that the distance histogram is similar to a unimodal distribution, which means that distances near the peak account for a larger proportion and have no certain semantic information as the criteria for similar or dissimilar. According to the theory of confidence interval, we set the weights for confident pairs to 1, whose corresponding distances are far away from the peak. To be specific, we set two distance thresholds d_l and d_r , and distances between d_l and d_r have a lower confidence. Note that for the fuzzy pairs ($\hat{S}_{ij} = 0$), the weight is set to 0. Therefore, confidence-based weight matrix is computed as following:

$$W_{ij} = \begin{cases} \frac{(t-d_{ij})^2}{(t-d_l)^2} & d_l < d_{ij} \leq t \& \hat{S}_{ij} \neq 0, \\ \frac{(d_r-t)^2}{(d_r-d_l)^2} & t < d_{ij} < d_r \& \hat{S}_{ij} \neq 0, \\ 1 & d_{ij} \leq d_l \mid d_{ij} \geq d_r \& \hat{S}_{ij} \neq 0, \\ 0 & \hat{S}_{ij} = 0 \end{cases} \quad (4)$$

where the smaller the distance d_{ij} , the greater the weight is for each unconfident similar pair ($t < d_{ij} < d_r$), while the larger the distance d_{ij} , the greater the weight is for each unconfident dissimilar pair ($d_l < d_{ij} \leq t$). In this way, the unconfident signals are down-weighted for smooth guidance.

Consistency Learning

For the purpose of preserving the similarity structure of input images, similar (dissimilar) images are expected to be mapped into similar (dissimilar) hash codes. Different from previous models, here we adopt two groups of semantic information under two different kinds of data augmentation.

Semantic Consistency For each image x_i , there are two transformed samples $x_i^{(1)}$ and $x_i^{(2)}$. At the semantic information generating stage, two refined similarity graphs with confidence matrices $\{W^{(1)}, \hat{S}^{(1)}\}$, $\{W^{(2)}, \hat{S}^{(2)}\}$ are generated with extracted features $\{F(x_i^{(1)})\}_{i=1}^N$ and $\{F(x_i^{(2)})\}_{i=1}^N$ as the guiding information. Simultaneously, images $x_i^{(1)}$ and $x_i^{(2)}$ are the inputs of the hashing network $G(\cdot)$, and hash codes $b_i^{(1)}$ and $b_i^{(2)}$ are obtained through activation function $sign(\cdot)$. Therefore, we derive two similarity outputs $H^{(1)}$ and $H^{(2)}$ from hash codes, which is formulated as

$$H_{ij}^{(m)} = \frac{1}{L} b_i^{(m)\top} b_j^{(m)}, \quad b_i^{(m)} = sign(G(x_i^{(m)}; \Theta)) \quad (5)$$

in which $m = 1$ or 2 , and Θ represents the set of parameters of hashing network. To preserve the semantic structures, we first minimize weighted L_2 loss between the hash code similarity and the corresponding pseudo-graph from the same group. In formulation,

$$\begin{aligned} \mathcal{L}_{parallel} = & \frac{1}{N^2} \sum_{i=1}^N \sum_{j=1}^N W_{ij}^{(1)} (H_{ij}^{(1)} - \hat{S}_{ij}^{(1)})^2 \\ & + W_{ij}^{(2)} (H_{ij}^{(2)} - \hat{S}_{ij}^{(2)})^2 \end{aligned} \quad (6)$$

Inspired by the cross-attention mechanism (Boussaha et al. 2019), we also match the hash code similarity with the pseudo-graph from the different group. To be specific,

$$\begin{aligned} \mathcal{L}_{cross} = & \frac{1}{N^2} \sum_{i=1}^N \sum_{j=1}^N W_{ij}^{(1)} (H_{ij}^{(2)} - \hat{S}_{ij}^{(1)})^2 \\ & + W_{ij}^{(2)} (H_{ij}^{(1)} - \hat{S}_{ij}^{(2)})^2 \end{aligned} \quad (7)$$

Contrastive Consistency Generally, ideal hashing methods generate hash codes with fewer collisions. From this points, we also preserve the consistency of hash codes from different augmentation through contrastive learning. To be specific, we randomly sample a minibatch of M images, producing $2M$ transformed images $\{x_i^{(1)}, x_i^{(2)}\}_{i=1}^M$. Given a positive pair $x_i^{(1)}$ and $x_i^{(2)}$, we treat the other $2(M-1)$ augmented images within a minibatch as negative examples. The contrastive consistency of the hash code of x_i is defined as

$$\begin{aligned} \ell_i = & -\frac{1}{2} \left(\log \frac{\exp(\cos(b_i^{(1)}, b_i^{(2)})/\tau)}{Z_i^{(1)}} \right. \\ & \left. + \log \frac{\exp(\cos(b_i^{(1)}, b_j^{(2)})/\tau)}{Z_i^{(2)}} \right) \end{aligned} \quad (8)$$

where

$$Z_i^{(m)} = \sum_{j \neq i} \exp(\cos(b_i^{(m)}, b_j^{(1)})/\tau) + \exp(\cos(b_i^{(m)}, b_j^{(2)})/\tau),$$

$m = 1$ or 2 , and τ denotes a temperature parameter set to 0.5 following (Chen et al. 2020). Note that the numerator of each term punishes the distance between hash codes of samples under different transformation while the denominator encourages to enlarge the distance between hash codes of different samples and thus alleviates collisions. The contrastive consistency loss computed across all images in a mini-batch is

$$\mathcal{L}_{contrastive} = \frac{1}{M} \sum_{i=1}^M \ell_i \quad (9)$$

Finally, the loss of consistency learning is formulated as

$$\begin{aligned} \mathcal{L} = & \mathcal{L}_{matching} + \eta \mathcal{L}_{contrastive} \\ = & \mathcal{L}_{parallel} + \mathcal{L}_{cross} + \eta \mathcal{L}_{contrastive} \end{aligned} \quad (10)$$

in which η is a coefficient to balance different consistency loss. However, the $sign(\cdot)$ is in-differentiable at zero and the derivation of it will be zero for every non-zero input, with the result that the parameters of the hashing model will not be updated by the back-propagation algorithm when minimizing the Equation 10. Thus, we use $tanh(\cdot)$ to approximate the sign function and generate the approximate hash code $v_i^{(m)} = \tanh(G(x_i^{(m)}))$ to replace $b_i^{(m)}$ in loss function. Our loss function is optimized by the mini-batch standard stochastic gradient descent (SGD) method. The whole learning procedure is summarized in Algorithm 1.

Algorithm 1 CIMON’s Training Algorithm

Input: Training images $\mathcal{X} = \{x_i\}_{i=1}^N$;
The length of hash codes : L ;

Output: Parameters Θ for the neural network $G(\cdot)$;
Hash codes B for training images.

- 1: Generate two transformed images via data augmentation for each image: $\mathcal{X}^{(1)}$ and $\mathcal{X}^{(2)}$;
- 2: **for** $m = 1, 2$ **do**
- 3: Get pre-train features of $\mathcal{X}^{(m)}$ through $F(\cdot)$;
- 4: Construct the pseudo-graph $S^{(m)}$ by Equation 1;
- 5: Cluster pre-train features into K different groups by Spectral Clustering and construct refined pseudo-graph $\hat{S}^{(m)}$ by Equation 3;
- 6: Construct the confidence matrix $W^{(m)}$ by Equation 4;
- 7: **end for**
- 8: **repeat**
- 9: Sample M images from \mathcal{X} and obtain their augmentation to construct a mini-batch;
- 10: Calculate the outputs by forward-propagating through the network $G(\cdot)$;
- 11: Update parameters of $G(\cdot)$ through back propagation by Equation 10;
- 12: **until** convergence

Experiments

We implement extensive experiments on several benchmark datasets to evaluate our CIMON by comparisons with several state-of-the-art unsupervised hashing methods.

Table 1: MAP for different methods on FLICKR25K, CIFAR-10 and NUSWIDE.

Methods	FLICKR25K				CIFAR-10				NUS-WIDE			
	16bits	32bits	64bits	128bits	16bits	32bits	64bits	128bits	16bits	32bits	64bits	128bits
ITQ	0.6492	0.6518	0.6546	0.6577	0.1942	0.2086	0.2151	0.2188	0.5270	0.5241	0.5334	0.5398
SH	0.6091	0.6105	0.6033	0.6014	0.1605	0.1583	0.1509	0.1538	0.4350	0.4129	0.4062	0.4100
DSH	0.6452	0.6547	0.6551	0.6557	0.1616	0.1876	0.1918	0.2055	0.5123	0.5118	0.5110	0.5267
SpH	0.6119	0.6315	0.6381	0.6451	0.1439	0.1665	0.1783	0.1840	0.4458	0.4537	0.4926	0.5000
SGH	0.6362	0.6283	0.6253	0.6206	0.1795	0.1827	0.1889	0.1904	0.4994	0.4869	0.4851	0.4945
DeepBit	0.5934	0.5933	0.6199	0.6349	0.2204	0.2410	0.2521	0.2530	0.3844	0.4341	0.4461	0.4917
SSDH	0.7240	0.7276	0.7377	0.7343	0.2568	0.2560	0.2587	0.2601	0.6374	0.6768	0.6829	0.6831
DistillHash	-	-	-	-	0.2844	0.2853	0.2867	0.2895	-	-	-	-
CUDH	0.7332	0.7426	0.7549	0.7561	0.2856	0.2903	0.3025	0.3000	0.6996	0.7222	0.7451	0.7418
MLS ³ RDUH	0.7587	0.7754	0.7870	0.7927	0.2876	0.2962	0.3139	0.3117	0.7056	0.7384	0.7629	0.7818
CIMON	0.8047	0.8198	0.8282	0.8319	0.4576	0.4802	0.5019	0.4984	0.7893	0.8058	0.8204	0.8241

Datasets and Setup

FLICKR25K (Huiskes and Lew 2008) contains 25,000 images collected from the Flickr website. Each image is manually annotated with at least one of the 24 unique labels provided. We randomly select 2,000 images as the query set. The remaining images are used as the retrieval set, and 10000 images are randomly selected from the retrieval set as the training set.

CIFAR-10 (Krizhevsky, Hinton et al. 2009) contains 60K images of 10 different categories. For each class, we randomly select 1,000 images as the query set and take the rest as the database. We sample 500 images per class in the database as the training set.

NUSWIDE (Chua et al. 2009) contains 269,648 images, each of the images is annotated with multiple labels referring to 81 concepts. The subset containing the 10 most popular concepts is used here. We randomly select 5,000 images as the query set and the remaining images make up the database. 5000 images are randomly selected from the database as the training set.

STL-10 (Coates, Ng, and Lee 2011) contains 500(800) training(test) images from each of 10 classes. All the training images are used for both training and retrieval. All the test images make up the query set.

Our method is compared with state-of-the-art unsupervised hashing methods including traditional methods and deep learning methods. Traditional methods includes ITQ (Gong et al. 2012), SH (Weiss, Torralba, and Fergus 2009), DSH (Jin et al. 2013), SpH (Heo et al. 2012) and SGH (Dai et al. 2017). Deep unsupervised hashing methods include DeepBits (Lin et al. 2016), SSDH (Yang et al. 2018), DistillHash (Yang et al. 2019), CUDH (Gu et al. 2019), and MLS³RUDH¹ (Tu, Mao, and Wei 2020). For deep learning-based methods, we use raw pixels as inputs. For traditional methods, we extract 4096-dimensional feature vectors by the VGG-F model which is pre-trained on ImageNet for fair comparison.

The ground-truth similarity information for evaluation is constructed from the ground-truth image labels: two data points are considered similar if they share the same label (for CIFAR-10 and STL-10) or share at least one common la-

bel (for FLICKR25K and NUSWIDE). The retrieval quality is evaluated by Mean Average Precision (MAP), Precision-Recall curve and Top N precision curve. MAP is a widely-used criteria to evaluate the retrieval accuracy. Given a query and a list of R ranked retrieval results, the average precision (AP) for the given query can be computed. MAP is defined as the average of APs for all queries. For datasets FLICKR25K and NUSWIDE, we set R as 5000 for the experiments. For CIFAR-10 and STL-10, R is set to the number of images in the database, 50000 and 5000 respectively. Precision-recall curve reveals the precision at different recall levels and is a good indicator of overall performance. Top N precision curve, which is the precision curve with respect to the top K retrieved instances, also visualizes the performance from a different perspective.

Implementation Details

The framework is implemented by Pytorch V1.4 and we optimize our model by mini-batch SGD with momentum. The mini-batch size is set to 24. The learning rate is fixed at 0.001. For all three datasets, training images are resized to 224×224 as inputs. Data augmentation we adopt includes random cropping and resizing, rotation, cutout, color distortion and Gaussian blur. As guided in (Wu et al. 2019), the distance threshold t is set to 0.1. The threshold d_l and d_r are selected as indicated in (Yang et al. 2018). As two introduced hyper-parameters, η and the number of clusters K in spectral clustering are set to 0.3 and 70 as default.

Experimental Results

Table 1 shows the MAPs of different methods on datasets FLICKER25K, CIFAR-10 and NUSWIDE with hash code lengths varying from 16 to 128. According to the results, the following observations can be derived:

- The performance of deep learning-based algorithms is overall better than traditional methods, which shows that the strong representation-learning ability of deep learning helps to improve the performance of unsupervised hashing method.
- The methods that reconstruct semantic similarity structure with global information (CUDH, MLS³RUDH) perform better than other deep unsupervised hashing methods,

¹Codes provided by the authors

which indicates that semantic similarity reconstructed only by local information (i.e. pairwise distance of features) is inaccurate and unreliable.

- We can find that CIMON has a significant improvement over the previous the-state-of-art MLS³RDUH in all cases by a large margin. Specifically, the improvements of our model over the best baseline are 5.51%, 60.25% and 8.39% for average MAP on datasets FLICKER25K, CIFAR-10 and NUS-WIDE respectively, which shows the superiority of our model.

Table 2: MAP for different deep hashing methods on STL-10.

Methods	STL-10			
	16bits	32bits	64bits	128bits
SSDH	0.4447	0.4558	0.4612	0.4497
CUDH	0.5010	0.5383	0.6378	0.6108
MLS ³ RDUH	0.6000	0.6266	0.6595	0.6646
CIMON	0.7243	0.7595	0.7717	0.7721

To fully explore the performance of our model on single-labeled dataset, we further study the performance of our model on STL-10 compared with three best baselines, and get the consistent results, which are shown in Table 2.

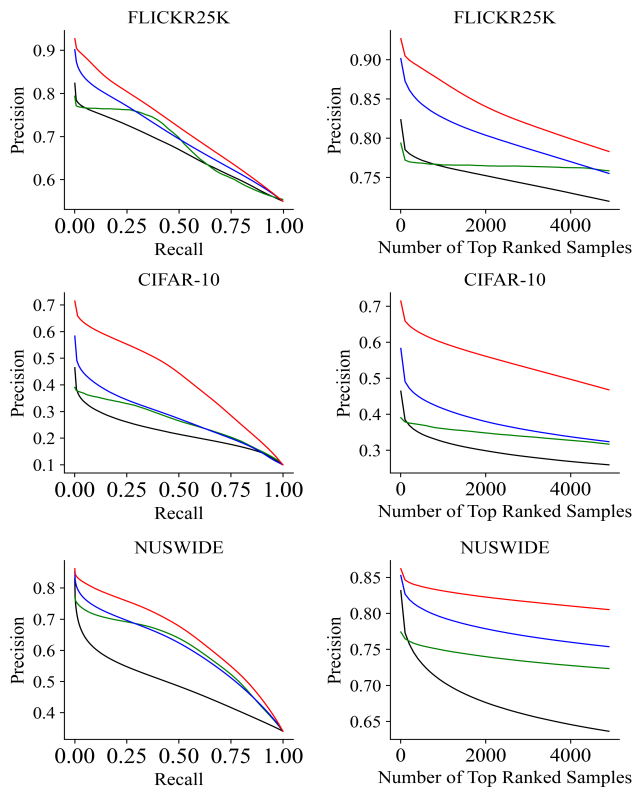


Figure 3: The first column plots the precision-recall curves, and the second column plots the Top- N precision curves. ($L = 128$, — SSDH, — CUDH, — MLS³RDUH, — CIMON)

We also plot the precision-recall curves of SSDH, CUDH, MLS³RDUH and CIMON on datasets FLICKR25K, CIFAR-10 and NUSWIDE, respectively, which are shown in the first column of Figure 3. It can be clearly seen that the curve of CIMON is always on top of the other three models' curves, which implies that the hash codes obtained by CIMON are also more suitable for hash table lookup search strategy. The second column of Figure 3 shows that the Top- N precision curves of these four models on the same datasets. The proposed CIMON significantly outperforms the comparison methods by large margins. Since the precision curves are based on the ranks of Hamming distance, CIMON is able to achieve superior performance under Hamming ranking-based evaluations.

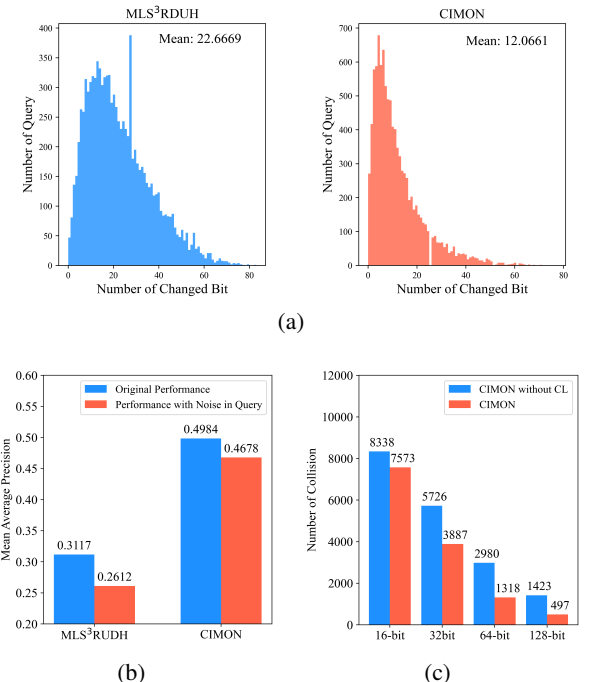


Figure 4: (a) Distribution of changed bits number after adding noise in query images on CIFAR-10 for MLS³RDUH and CIMON, respectively. (b) MAP results before and after adding noise to MLS³RDUH and CIMON. (c) The number of collisions in the query dataset for CIMON without contrastive consistency and CIMON.

Robustness. We add perturbation or transformation noise in the query set, which doesn't break the semantic information. Figure 4 (a) shows the distribution of changed bits number before and after adding noise in query images on CIFAR-10 for the best baseline and our model. It is observed that our model has better transformation invariant compared with the baseline. The MAP after the noise attack also decreases less compared with the baseline in Figure 4 (b).

Fewer Collisions. Figure 4 (c) shows the number of collisions in the query dataset for our model with contrastive consistency or not. It can be found that our full model suffer the fewer collisions, which implies that contrastive consis-

tency helps to generate high-quality hash codes with fewer collisions.

Ablation study

Table 3: Ablation analysis on CIFAR-10. GCL, CW, SC and CC correspond to Global Constraint Learning, Confidence-based Weight, Semantic Consistency and Contrastive Consistency, respectively.

	Correlations				Results			
	GCL	CW	SC	CC	16bits	32bits	64bits	128bits
M_1					0.1907	0.2253	0.2428	0.2592
M_2	✓				0.2103	0.2548	0.2645	0.2797
M_3	✓	✓			0.3225	0.3241	0.3453	0.3464
M_4	✓	✓	✓		0.3818	0.4345	0.4409	0.4455
M_5	✓	✓	✓	✓	0.4576	0.4802	0.5019	0.4984

We investigate the effectiveness of various correlations from four aspects: Global Constraint Learning, Confidence-based Weight, Cross Similarity Matching and Contrastive Learning in this section. The results are shown in Table 3.

Global Constraint Learning The only difference between M_2 and M_1 lies in whether to use the the global constraint learning to refine the pseudo similarity graph or not. It can be seen that M_2 surpasses M_1 significantly, which demonstrates the effectiveness of global constraint learning for reconstructing the accurate similarity graph.

Confidence-based Weight After considering the confidence of semantic similarity, M_3 achieves much better result than M_2 under all settings. Specifically, there is a 14.62% improvement with 128-bits code length. The reason is that the refined similarity-graph is still noisy and M_4 further accounts for the variations in confident and unconfident pairs, which eases the effect of false similarity signals and enlarges the effect of highly confident signals in similarity graph.

Semantic Consistency M_4 makes use of the data augmentation and our novel semantic consistency loss function, while M_3 only matches the hash codes similarity and pseudo-similarity graph derived from original images. We can see that M_4 performs much better than M_3 , which demonstrates the strength of data augmentation and our well-designed semantic consistency loss.

Contrastive Consistency By comparing the results of M_5 and M_4 , we can see that the contrastive consistency can further improve the performance of our model. As we analyzed in Figure 4, with the help of contrastive learning, our model can not only generate the hash codes with fewer collisions, but also improve the robustness of the hash codes to various noise. So it can further improve the result.

Parameter Sensitivity

We further study the influence of hyper-parameter η and the number of clusters K . Figure 5 shows the effect of these two hyper-parameters on CIFAR-10 with 128 bits code length. We first fix η to 0.1 and 0.3 and evaluate the MAP by varying the number of clusters from 50 to 110. The performance of model is not sensitive to the number of clusters in the range of [50, 110] and we can set K as any values in that interval.

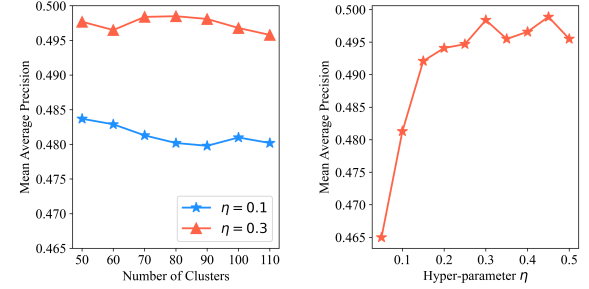


Figure 5: Sensitivity of η and number of clusters with 128-bits on CIFAR-10

Furthermore, we show the MAP by varying η from 0.05 to 0.5 with K fixed to 70. MAP of our model first increases and then keeps at a relatively high level. The result is also not sensitive to η in the range of [0.2, 0.5]. Then for the proposed model, K and η are set to 70 and 0.3 respectively.

Visualization

Query	Top-10 Retrieved Images										CIMON P@10 100%
	1	2	3	4	5	6	7	8	9	10	
Car											MLS-RUDH P@10 50%
	✓	✓	✓	✓	✓	✓	✓	✓	✓	✓	
Horse											CIMON P@10 90%
	X	✓	✓	✓	✓	✓	✓	✓	✓	✓	
Ship											MLS-RUDH P@10 10%
	✓	✓	✓	✓	✓	✓	✓	✓	✓	✓	

Figure 6: Examples of the top 10 images and Precision@10 on CIFAR-10

In Figure 6, we visualize the top 10 returned images of our model and the best baseline for three query images of CIFAR-10, which demonstrates that our model can retrieve much more relevant and user-desired images.

Conclusion

In this paper, we propose a novel deep hashing method named CIMON, which first generates reliable semantic information by comprehensive similarity mining from local and global views. Then a novel consistency loss function from the view of semantic matching and contrastive learning is proposed to optimize the hashing model by incorporating the semantic information into the training process. Extensive experiments reveal that CIMON remarkably boosts the state-of-the-art unsupervised hashing schemes in both image retrieval and robustness.

References

Boussaha, B. E. A.; Hernandez, N.; Jacquin, C.; and Morin, E. 2019. Multi-level Context Response Matching in Retrieval-Based Dialog Systems. In *Proceedings of the 7th edition of the Dialog System Technology Challenges Workshop at AAAI*.

Cao, Y.; Long, M.; Liu, B.; and Wang, J. 2018. Deep cauchy hashing for hamming space retrieval. In *Proceedings of the IEEE Conference on Computer Vision and Pattern Recognition*, 1229–1237.

Chen, T.; Kornblith, S.; Norouzi, M.; and Hinton, G. 2020. A simple framework for contrastive learning of visual representations. *arXiv preprint arXiv:2002.05709* .

Chua, T.-S.; Tang, J.; Hong, R.; Li, H.; Luo, Z.; and Zheng, Y. 2009. NUS-WIDE: a real-world web image database from National University of Singapore. In *Proceedings of the ACM international Conference on Image and Video Retrieval*, 48.

Coates, A.; Ng, A.; and Lee, H. 2011. An analysis of single-layer networks in unsupervised feature learning. In *Proceedings of the fourteenth International Conference on Artificial Intelligence and Statistics*, 215–223.

Dai, B.; Guo, R.; Kumar, S.; He, N.; and Song, L. 2017. Stochastic generative hashing. In *Proceedings of the 34th International Conference on Machine Learning-Volume 70*, 913–922.

Dosovitskiy, A.; Springenberg, J. T.; Riedmiller, M.; and Brox, T. 2014. Discriminative Unsupervised Feature Learning with Convolutional Neural Networks. In Ghahramani, Z.; Welling, M.; Cortes, C.; Lawrence, N. D.; and Weinberger, K. Q., eds., *Advances in Neural Information Processing Systems 27*, 766–774.

Gong, Y.; Lazebnik, S.; Gordo, A.; and Perronnin, F. 2012. Iterative quantization: A procrustean approach to learning binary codes for large-scale image retrieval. *IEEE Transactions on Pattern Analysis and Machine Intelligence* 35(12): 2916–2929.

Gu, Y.; Wang, S.; Zhang, H.; Yao, Y.; and Liu, L. 2019. Clustering-driven unsupervised deep hashing for image retrieval. *Neurocomputing* 368: 114–123.

Hadsell, R.; Chopra, S.; and LeCun, Y. 2006. Dimensionality reduction by learning an invariant mapping. In *2006 IEEE Computer Society Conference on Computer Vision and Pattern Recognition*, volume 2, 1735–1742.

He, K.; Fan, H.; Wu, Y.; Xie, S.; and Girshick, R. 2020. Momentum contrast for unsupervised visual representation learning. In *Proceedings of the IEEE/CVF Conference on Computer Vision and Pattern Recognition*, 9729–9738.

Heo, J.-P.; Lee, Y.; He, J.; Chang, S.-F.; and Yoon, S.-E. 2012. Spherical hashing. In *2012 IEEE Conference on Computer Vision and Pattern Recognition*, 2957–2964.

Huiskes, M. J.; and Lew, M. S. 2008. The MIR flickr retrieval evaluation. In *Proceedings of the 1st ACM international conference on Multimedia information retrieval*, 39–43.

Jin, Z.; Li, C.; Lin, Y.; and Cai, D. 2013. Density sensitive hashing. *IEEE transactions on cybernetics* 44(8): 1362–1371.

Krizhevsky, A.; Hinton, G.; et al. 2009. Learning multiple layers of features from tiny images .

Li, Q.; Sun, Z.; He, R.; and Tan, T. 2017. Deep supervised discrete hashing. In *Advances in Neural Information Processing Systems*, 2482–2491.

Lin, K.; Lu, J.; Chen, C.-S.; and Zhou, J. 2016. Learning compact binary descriptors with unsupervised deep neural networks. In *Proceedings of the IEEE Conference on Computer Vision and Pattern Recognition*, 1183–1192.

Luo, X.; Chen, C.; Zhong, H.; Zhang, H.; Deng, M.; Huang, J.; and Hua, X. 2020. A Survey on Deep Hashing Methods. *arXiv preprint arXiv:2003.03369* .

Simonyan, K.; and Zisserman, A. 2015. Very Deep Convolutional Networks for Large-Scale Image Recognition. In *International Conference on Learning Representations*.

Tu, R.-C.; Mao, X.-L.; and Wei, W. 2020. MLS3RDUH: Deep Unsupervised Hashing via Manifold based Local Semantic Similarity Structure Reconstructing. In Bessiere, C., ed., *Proceedings of the Twenty-Ninth International Joint Conference on Artificial Intelligence*, 3466–3472.

Weiss, Y.; Torralba, A.; and Fergus, R. 2009. Spectral Hashing. In Koller, D.; Schuurmans, D.; Bengio, Y.; and Bottou, L., eds., *Advances in Neural Information Processing Systems 21*, 1753–1760.

Wu, J.; Long, K.; Wang, F.; Qian, C.; Li, C.; Lin, Z.; and Zha, H. 2019. Deep comprehensive correlation mining for image clustering. In *Proceedings of the IEEE International Conference on Computer Vision*, 8150–8159.

Wu, Z.; Xiong, Y.; Yu, S. X.; and Lin, D. 2018. Unsupervised feature learning via non-parametric instance discrimination. In *Proceedings of the IEEE Conference on Computer Vision and Pattern Recognition*, 3733–3742.

Yang, E.; Deng, C.; Liu, T.; Liu, W.; and Tao, D. 2018. Semantic structure-based unsupervised deep hashing. In *Proceedings of the 27th International Joint Conference on Artificial Intelligence*, 1064–1070.

Yang, E.; Liu, T.; Deng, C.; Liu, W.; and Tao, D. 2019. Distillhash: Unsupervised deep hashing by distilling data pairs. In *Proceedings of the IEEE Conference on Computer Vision and Pattern Recognition*, 2946–2955.

Zelnik-manor, L.; and Perona, P. 2005. Self-Tuning Spectral Clustering. In Saul, L. K.; Weiss, Y.; and Bottou, L., eds., *Advances in Neural Information Processing Systems 17*, 1601–1608.